Article

Copper-containing catalysts for azide-alkyne cycloaddition in supercritical CO₂

Sonia López [1], Jesús Manuel García-Vargas [1], María Teresa García [1], Juan Francisco Rodríguez [1], Ignacio Gracia [1] and María Jesús Ramos [1], *

[1] Institute of Chemical and Environmental Technology (ITQUIMA), Department of Chemical Engineering, University of Castilla- La Mancha, Avda. Camilo José Cela 1A, 13071 Ciudad Real, Spain.

* Correspondence: mariajesus.ramos@uclm.es; Tel.: +34926295300

Abstract:

Background: Chemical industry has increased the investment and innovation capacity to supply chemicals from safe and sustainable sources, which will be essential to offer new solutions and support the green transition of the global economy and society. In this sense, the use of green solvents and reusable heterogeneous catalysts have emerged as a promising sustainable process strategy for engineering, chemistry and the environment. In this work, different homogeneous (copper bromide, CuBr and copper(II) acetate, Cu (CH₃COO)₂·H₂O) and heterogeneous (Cu Wire, Cu Plate, Cu/β-SiC, pre-treated Cu Wire and pre-treated Cu Plate) copper catalysts have been tested for the copper(I)-catalyzed alkyne-azide cycloaddition (CuAAC) reaction. In addition, the influence of different reaction media has been analyzed, comparing the use of an organic solvent like toluene and a green solvent like supercritical CO₂ (scCO₂).

Methods: Characterization of the catalysts include X-ray diffraction (XRD), Scan Electron Microscope (SEM), Atomic absorption spectrophotometry (AA) and Temperature Programmed Reduction (TPR). Parameters such as catalyst loading, reaction time, reusability and leaching of the catalysts were studied to obtain more information on the CuAAC reaction in scCO₂.

Results: Pre-treated copper plate achieved a 57 % increase in reaction yield compared to non pre-treated copper plate. However, the recovery and reuse of pre-treated copper plate showed a severe deterioration and a considerable change in its surface. Cu Wire (without pre-treatment) achieved yields of up to 94.2 % after reusing it for five cycles.

Conclusions: These results open the possibility to exploit the combination of heterogeneous catalysts and scCO₂ and justify further research to highlight green solvents and simultaneously address the challenges of reaction, purification and recycling.

Keywords: CuAAC; Copper catalysts; scCO₂, green chemistry, heterogeneous catalyst, reusability.

Publisher's Note: MDPI stays neutral with regard to jurisdictional claims in published maps and institutional affiliations.

1. Introduction.

Cycloaddition using azides and alkynes is an important method for the synthesis of 1,2,3 triazoles, which was firstly reported by Huisgen et al. in 1960 [1]. A particular case of this process is the copper-catalyzed alkyne-azide cycloaddition (CuAAC). The reaction kinetics and mechanism for the CuAAC reaction have been studied in detail since its discovery in 2002 [2,3]. The Cu (+1) catalysis has transformed this cycloaddition into an essentially quantitative and regioselective click reaction, as developed by the Sharpless and Meldal laboratories [2–5]. The CuAAC reaction is generally considered as the most prolific and successful click reaction in drug discovery, bioconjugation applications, and

polymer chemistry. CuAAC reaction has found wide application due to its simplicity, applicability and efficiency and is based on the formation of 1,4-disubstitued 1,2,3-triazoles between a terminal alkyne and an aliphatic or aromatic azide in the presence of copper [5–8].

The first example of CuAAC was carried out in water/t-BuOH at room temperature [9]. However, CuAAC reaction is habitually carried out with organic solvents in terms of polymer and organic chemistry as reaction media, such as N, N dimethylformamide (DMF), toluene or tetrahydrofuran (THF) [10–11]. Traditional organic solvents could potentially cause various health and environmental issues due to their volatility and toxicity, so the reduction of its use is encouraged by the nowadays social concern and political regulations. In the past few decades, the use of supercritical fluids (SCFs) as an alternative to the use of traditional organic solvents for chemical synthesis has attracted huge attention [12,13]. Among all SCFs, $scCO_2$ has received special interest as it is nontoxic, nonflammable, inexpensive and easy to dispose and recycle [14,15].

CuAAC click reactions have been explored and analyzed in many different green solvents and reaction media, including $scCO_2$. In 2009, Grignard et al. [16,17] reported the first example of modification of aliphatic polyesters via CuAAC in $scCO_2$ and the removal of the catalyst (CuI) using $scCO_2$ extraction. Later, the same authors prepared a polymer with a chain-end functionality through CuAAC in $scCO_2$. In 2015, Zhang et al. [18] developed an efficient protocol for the CuAAC catalyzed by $Cu(CH_3COO)_2 \cdot H_2O$ in supercritical carbon dioxide in absence of ligand. A recent work from our group [19] showed the viability of CuAAC with a polyether in $scCO_2$ using acetate of copper monohydrate as catalyst. To the best of our knowledge, only four papers can be found in literature where the CuAAC reaction is studied using $scCO_2$ as reaction media.

Regarding the catalyst, a wide variety of copper catalysts can be used in CuAAC reaction as long as Cu (+1) ion species are generated [10,20-22]. There are three general methodologies to ensure the presence of Cu (+1) ions in the reaction medium, that can be selected depending on the experimental conditions of the reaction. The first one of these strategies is in-situ reduction of copper (II) salts, commonly using copper sulphate pentahydrate and sodium ascorbate as a reducing agent [23,24]. The second strategy is the oxidation of metallic copper and the last one is the addition of copper (I) salts directly. Sometimes, this last strategy is coupled with the addition of certain nitrogen bases or ligands such as N, N-diisopropylethylamine (DIPEA) or N,N,N′,N′′,N′′-Pentamethyl diethylenetriamine (PMDTA), which are able to stabilize the oxidation state +1 of the copper and promote the reaction by reducing the formation of by-products [25,26]. Patricia L. Golas et al. [27], studied different catalyst and ligands, observing that tridentate amine ligands produced faster reaction rates than pyridine-based ligands, being the first ones the most effective ligands in CuAAC.

A new catalysis strategy is currently being developed and studied in the green chemistry context: heterogeneous catalysis in CuAAC. The main benefits attributed to this mode of reaction are the simplicity of processing, recyclability (catalysts preserve their activity throughout several reaction cycles) and minimization of waste, which means a reduction in environmental concerns [21].

There are a great variety of works that have studied different heterogeneous copper catalysts using organic solvents and high temperatures in the CuAAC reaction [11,28-31]. However, there are only two recent papers where a heterogeneous copper catalyst was used in the CuAAC reaction in $scCO_2$; and a copper wire was selected as catalyst for both studies [32,33]. Nevertheless, these works did not study in depth the behavior of this catalyst in $scCO_2$. Therefore, the CuAAC reaction in $scCO_2$ is yet far from being fully understood.

In this study the reaction between methoxy polyethylene glycol (mPEG-alkyne) and coumarin with azide group was selected as a model of the cycloaddition reaction in order to study the influence on CuAAC of different catalysts and reaction media (Scheme 1). This conjugate can be used in pharmaceutical applications, as it was found to be able to

form nanoaggregates to form micelles and also exhibits anti-oxidative capacity and fluorescent characteristics for monitoring of disease treatment provided by coumarin [34]. Optimal conditions of pressure and temperature of scCO2 for the CuAAC reaction were fixed after the previous optimization study [35]. Both homogeneous and heterogeneous catalysts were considered for this work. The homogeneous catalysts selected were CuBr and $Cu(CH_3COO)_2 \cdot H_2O$ and the heterogeneous catalysts were Cu Wire, Cu Plate, Cu/β-SiC, Pre-treated Cu Wire and Pre-treated Cu Plate. Silicon carbide pellets (β-SiC) have been widely employed as catalytic support for heterogeneous catalysis, as it exhibits a high thermal conductivity, a high resistance towards oxidation, a high mechanical strength, chemical inertness, and average surface area [35–37]. In addition, this work also reports the reusability of the tested catalyst after several cycles in the CuAAC reaction in scCO2.
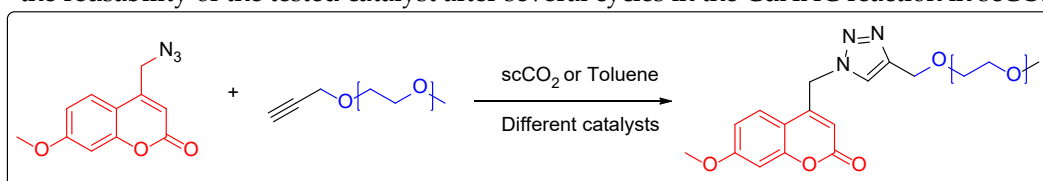
Scheme 1. Model CuAAC reaction.

2. Results and Discussion.

In this research, the reaction between mPEG-alkyne and coumarin-azide was selected as a model of the CuAAC, in order to study the influence of different copper catalysts and solvents. The results have been divided in four main sections. In the first place, mechanism of heterogeneous catalysts in scCO2 was analyzed at 13 MPa. In the second place, the influence of a catalyst pre-treatment was reported here in order to produce a new alternative to chemical synthesis routes. In the third section, we report a comparison of the yield values obtained for the click chemistry at atmospheric and high pressure with different copper catalyst. Finally, the recyclability and leaching were studied for heterogeneous catalysts.

2.1. Behaviour of copper catalyst in scCO2.

In this section, effect of scCO2 in the oxidation state of the catalysts were evaluated with XRD in order to better understand their behavior in the CuAAC reaction. Cu (+1), Cu (+2) oxides and Cu (0) species were observed in the copper catalysts, and their intensities compared for the different samples.

Figure 1 shows XRD spectra of acetate of copper monohydrate and copper bromide, before and after being exposed in scCO2 at 13 MPa and 24 hours. The peak positions of $Cu(CH_3COO)_2 \cdot H_2O$ at 12.56°, 14.20°, 16.30°, 20.34°, 24.84°, 25.64°, 33.27°, 34.79°, 36.49°, 38.72°, 40.88°, 44.37°, 46.39° , 50.92° , 55.97° , 58.19° , 63.97°, 66.4° and 69.73° are indexed as (110), (002), (11-2), (020), (202), (20-4), (312), (42-3), (13-3), (33-3), (42-5), (22-6), (53-3), (404), (045), (13-7), (060), (641) and (262) hkl planes having space group symmetry of C2/c (15) [37]. The peaks are in good conformity with the pure phase of the Joint committee on powder diffraction standards (JCPDS, PDF-14-0811). When the $Cu(CH_3COO)_2 \cdot H_2O$ was exposed to supercritical medium, the XRD profile changed (Figure 1 (a)). The exposure of $Cu(CH_3COO)_2-H_2O$ to scCO2 leads to the formation of several coexisting phases (Cu_2O and CuO). XRD showed the appearance of peaks at 29.46°, 36.29°, 42.15°, 61.13° attributed to Cu_2O and 25.68°, 57.89° attributed to CuO.

This fact indicates that scCO2 at 35 °C and 13 MPa modified the initial structure of $Cu(CH_3COO)_2 \cdot H_2O$ giving rise to copper species with different oxidation state which in very interesting result in order to achieve excellent yields of CuAAC reaction. In addition $Cu(CH_3COO)_2 \cdot H_2O$ has been used in scCO2 as catalyst [18,41].

Figure 1. (b) shows the XRD spectrum of the CuBr, which contains seven peaks that are clearly distinguishable. The prominent XRD peaks at 27.06°, 44.9°, 53.26°, 65.46°, 72.26°, 83.02° and 89.34° are indexed as (111), (220), (311), (400), (331), (422) and (481) hkl

planes having space group symmetry of F-43m (216) [39]. The peaks positions are in good 144
agreement with those for CuBr powder obtained from the International Center of Diffrac- 145
tion Data card (ICDD, formerly JCPDS, 06-0292). All of them can be perfectly indexed to 146
crystalline γ-CuBr, not only in peak position, but also in their relative intensity [42]. In 147
this case, no variation in the XRD profile was observed when copper bromide is exposed 148
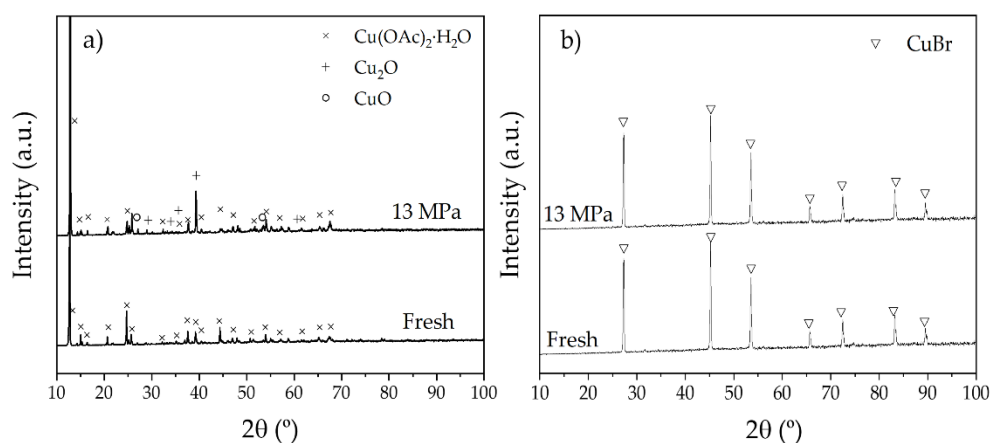to scCO$_2$ at 13 MPa. 149

150

151

Figure 1. XRD spectra of fresh catalysts and after scCO$_2$ at 13 MPa and 35 °C (a) Cu(CH$_3$COO)$_2$·H$_2$O 153
and (b)CuBr. 154

Figure 2 (a), (b) and (c) showed XRD spectra of Cu Wire, Cu Plate and Cu/β-SiC, fresh 155
catalysts and after being exposed in scCO$_2$ at 13 MPa, 35 °C and 24 hours. Cu Wire fresh 156
catalyst diffractogram illustrates that the peaks positions are in good conformity with the 157
pure cubic copper phase from the Joint Committee on Powder Diffraction Standards 158
(JCPDS, PDF-14-0811). No peaks attributable to possible impurities is observed. The XRD 159
peaks at 43.54°, 50.44°, 74.04°, 90.25° and 95.03° are indexed as (111), (200), (220), (311) and 160
(222) hkl planes having space group symmetry of Fm$\overline{3}$m (225). After exposure to scCO$_2$, 161
new peaks appear at 36.76°, 42.15° and 77.05° that correspond to Cu$_2$O and at 66.13° and 162
84.82° corresponding to CuO. Since the scCO$_2$ has been used in numerous works as an 163
oxidizing agent for heterogeneous catalyst [38,42], the formation of Cu$_2$O and CuO phases 164
on the surface of the copper wire could be explained by the effect of the exposure to this 165
compound. 166

The Figure 2 (b) shown the XRD of Cu Plate. The peaks at 43.54°, 50.44°, 74.04° and 167
90.25° are indexed as (111), (200), (220) and (311) hkl planes of Cu (0). No variation in the 168
XRD profile was observed when copper plate is exposed to scCO$_2$ at 13 MPa, thus scCO$_2$ 169
was not capable of oxidizing to oxidise the copper plate at these conditions, and therefore 170
did not generate the Cu (+1) ions, which are considered the most active copper specie for 171
the CuAAC. 172

Regarding to Cu/β-SiC, it was also evaluated its oxidation stability in scCO$_2$ (Figure 173
2 (c)). After the exposure to scCO$_2$ at 13 MPa and 35 °C for 24h, XRD patterns illustrate the 174
same crystalline structure of the SiC support, with peaks at 35.5°, 59.7°, 71.4°, 75.1° and 175
89.5° indexed as (111), (220), (311), (222) and (400) hlk planes having space group sym- 176
metry of F$\overline{43}$m (216). After impregnation of Cu species, the cubic SiC remains the main 177
peaks. The diffraction peaks of related with copper species catalyst were located at 43.3°, 178
50.4° and 74.1° coincide with the (111), (200) and (220) reflections of CuO respectively ac- 179
cording to JCPDS fiche 04-0836, verifying the presence of this element. Differences in the 180
XRD before and after scCO$_2$ exposure were not observed (Figure 2 (c)). 181

Therefore, it can be concluded that XRD of CuBr, Cu/β-SiC and Cu Plate catalysts did not reveal any variation in their structure after exposure to scCO$_2$. However, XRD profiles of Cu(CH$_3$COO)$_2$·H$_2$O and Cu Wire changed after contact with scCO$_2$ at 13 MPa and 35 °C for 24 h, giving rise to Cu$_2$O in Cu(CH$_3$COO)$_2$·H$_2$O and Cu$_2$O and CuO in Cu Wire, which indicates the ability of scCO$_2$ to modify the oxidation state of copper in these catalysts.
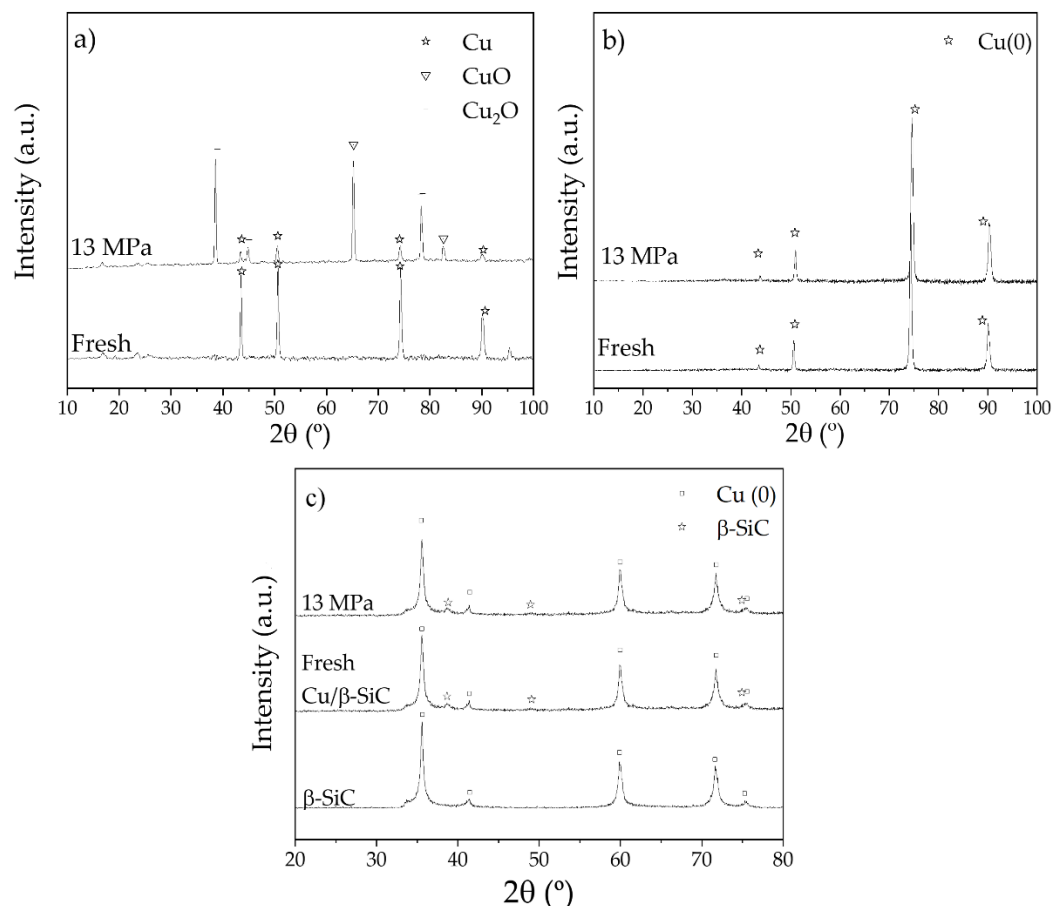

Figure 2. XRD spectra of fresh catalysts and after scCO$_2$ at 13 MPa and 35 °C (a) Cu Wire (b) Cu Plate and (c) Cu/β-SiC.

2.2. Pre-treament of Cu Wire and Cu Plate.

The pre-treatment was carried out with the main objective of undertaking the existence of copper with the oxidation state (+1) on the surface of these catalysts, in order to accelerate the reaction rate and to maintain the Cu (+1) concentration at a sufficient level during reaction. In this section, a simple and inexpensive synthesis approach was described for direct growth of Cu$_2$O and CuO in Cu Wire and Cu Plates.

In a first step, the pre-treatment conditions were settled according to temperature programmed reduction (TPR) test on Cu metal catalysts, which yielded information about the temperature for the transition from one copper oxide specie to another during the reduction process. Figure 3 shows the TPR profiles of Cu Wire and Cu Plate after previous oxidation.
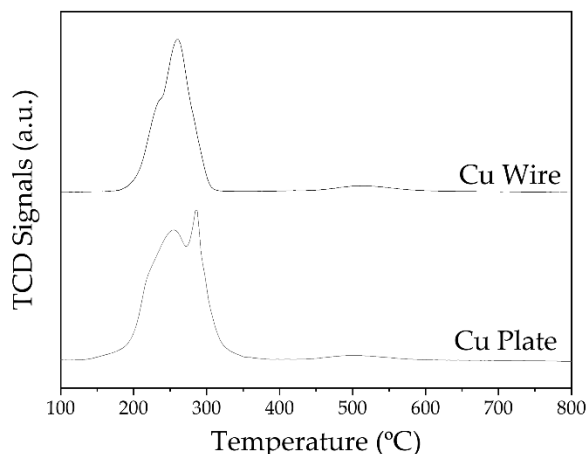
Figure 1. TPR profiles of Cu Wire and Cu Plate.

For both catalysts, it can be observed at low temperatures, between 200 °C and 400 °C, two reduction peaks. The first peak corresponds to the reduction of Cu (+2) to Cu (+1) and the second peak correspond to the reduction of Cu (+1) to Cu (0) [49,50]. The TPR curve of copper wire shows a higher intensity peak at 284.4 °C with a shoulder at 250 °C whereas for copper plate, the reduction profile shows a higher intensity peak at 245 °C with a shoulder at 285 °C. The two reduction peaks overlap in both catalysts, which implies that the transition from one specie to another occurs in a short temperature range.

Once the TPR was carried out, the pre-treatment protocol was stablished as follow. After loading the sample, an initial oxidation of the catalysts was carried out using synthetic air (10 mL/min) and heating the sample from room temperature up to 400 °C, at a rate of 6.67 °C/min. After reaching 400 °C, the sample was kept at these conditions for 120 minutes in order to oxidase most of the metal surface and produce CuO [50]. Secondly, with a stream of inert N_2 (50 mL/min) the temperature was reduced to 200 °C with a rate of 10 °C/min. Finally, the reduction of CuO to Cu_2O with H_2 (10 mL/min) took place at 200 °C for 30 minutes. The aim of this last step was to reduce the copper (+2) oxide species to copper (+1) according to the results of TPR. Figure 4 shows the XRD profile of Cu wire and Cu plate before and after pre-treatment.
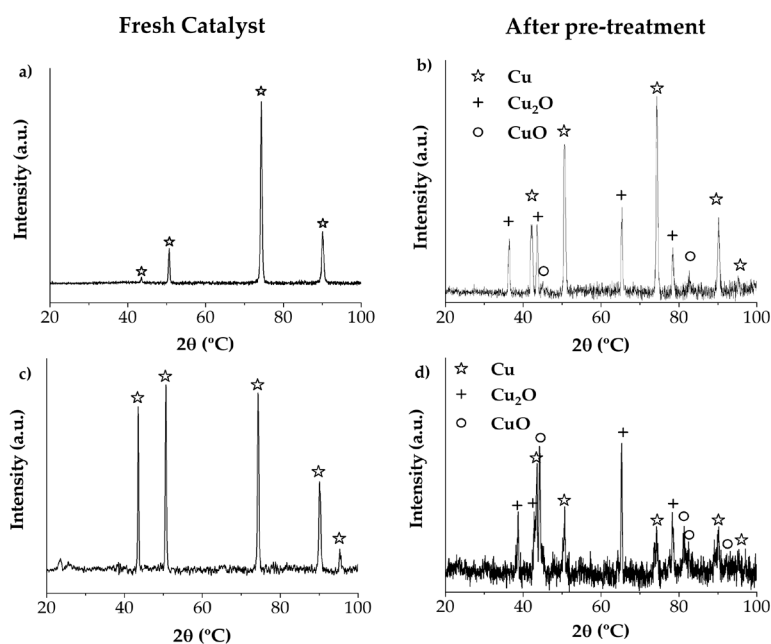
Figure 2. XRD spectra Cu Plate (a) fresh and (b) after pre-treated and Cu Wire (a) fresh and (b) after pre-treated.

XRD profiles of Cu Wire and Cu Plate before pre-treatment showed the peaks centred at about at 43.54°, 50.44°, 74.04° and 90.25°, attributed to the (111), (200), (220) and (311) hkl reflection planes respectively of pure metallic copper. It can be seen how the intensity corresponding to the pure copper peaks decreases after pre-treatment in both catalysts.

In the Figure 4 (d), Pre-treated Cu Wire, new peaks were identified at 36.7°, 42.78°, 65.74° and 76.9° assigned to Cu_2O and 44.95°, 81.09°, 82.17 and 92.92° assigned to CuO. Regarding to Pre-treated Cu Plate (Figure 4 (b)), it showed new peaks at 36.28°, 42.3°, 65.04° and 77.04° which are indexed as (111), (200), (220) and (311) hkl planes which correspond to Cu_2O and 44.35 and 82.62° which are attributed to CuO. Therefore, it is possible to confirm that the pre-treatment process contributes to the formation of Cu_2O and CuO species. Scan Electron Microscopy (SEM) characterization was carried out in order to study the morphology changes (Figure 5).
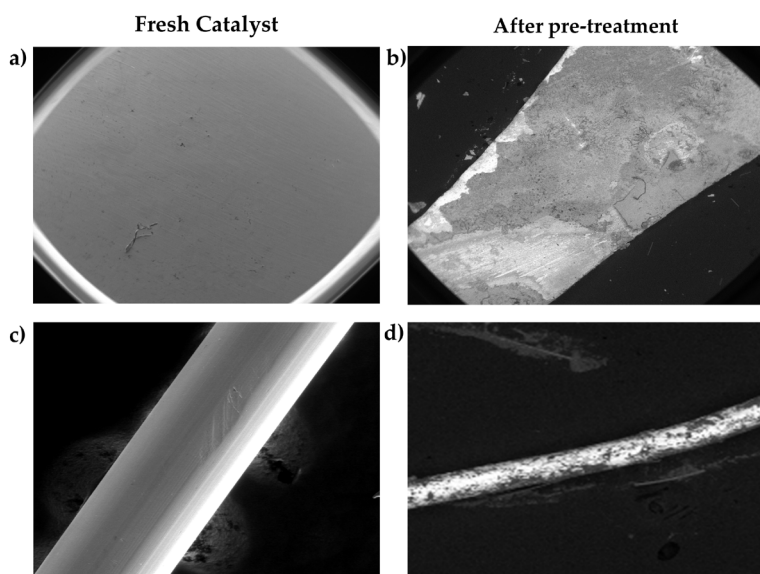
Fresh Catalyst **After pre-treatment**

235

Figure 3. SEM images Cu Plate *(*a) fresh and *(*b) after pre-treated and Cu Wire *(c)* 236
fresh and *(d)* after pre-treated. 237

238

In the SEM photographs, it is possible to observe that the surface of Cu Plate and Cu 239
Wire were oxidized to form appreciable Cu_2O and CuO crystals. However, the effect of 240
the pre-treatment was not uniform over the whole surface of the catalysts. Thus, it can be 241
concluded that both Cu (0), Cu_2O and CuO species coexist within the oxidized copper 242
plate and copper wire, being Cu_2O the dominant oxide after this pre-treatment. However, 243
it is quite clear from the comparison of both (pre-treated Cu Wire and Cu Plate), that in 244
the oxidation-reduction process of Cu Wire much species of CuO were generated com- 245
pared to copper plate. 246

247

2.3. CuAAC model reaction with different copper structures. 248

The activity of different copper catalysts in CuAAC with toluene and $scCO_2$ as sol- 249
vents was evaluated, as indicated the Figure 6, and the results obtained appear in this 250
section. 251
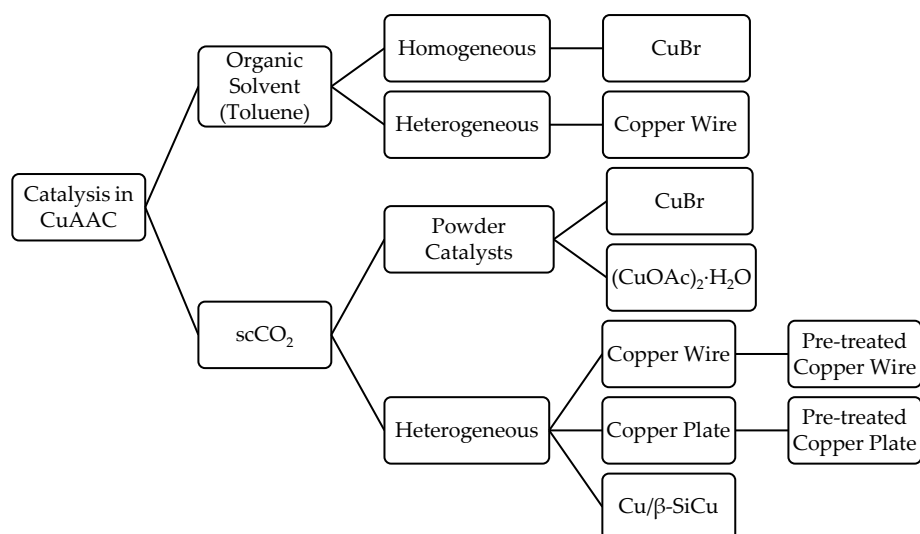
252

Figure 4. Chart of catalysts used in Toluene and scCO$_2$. 253

The coupling of mPEG alkyne with 4-azidomethyl-7-methoxycoumarin (AMMC) 254
using Toluene as solvent, different catalyst (CuBr and Cu Wire) and ligand or absence of 255
ligand was studied in the first place, and a summary of yield results is given in the Table 256
1. 257

Table 1. Yield of CuAAC reaction with different catalyst using an organic solvent 258

Entry	Copper Source	PMDTA (mmol)	Time (h)	Yield (%)
1	CuBr	-	6	0
2	CuBr	-	12	0
3	CuBr	-	24	0
4	CuBr	-	48	0
5	CuBr	0.05	6	33.6
6	CuBr	0.05	12	34.2
7	CuBr	0.05	24	43.18
8	CuBr	0.05	48	63.7
9	CuBr	0.025	24	11.48
10	Cu Wire	-	6	0
11	Cu Wire	-	12	0
12	Cu Wire	-	24	0
13	Cu Wire	-	48	0
14	Cu Wire	0.05	6	32.55
15	Cu Wire	0.05	12	42.91
16	Cu Wire	0.05	24	78.76
17	Cu Wire	0.05	48	91.92
18	Cu Wire	0.025	24	33.63

Coumarin Azide (0.05 mmol), mPEG-alkyne (0.05 mmol), CuBr (0.05 mmol), Cu Wire (100 mmol)
at 80 °C, anhydrous toluene and under inert atmosphere.

Using toluene as reaction media, the CuAAC reaction with CuBr as catalyst and no addition of PMDTA did not take place. The addition of PMDTA ligand significantly increased the conversion, reaching a yield of 63.7 % after 48 h at the considered conditions. The addition of half of the previous amount of PMDTA produced a slower rate of click product formation with a reduction in the yield values. The use of CuBr as catalyst could offer the potential to avoid the necessity of reducing agents, as in this salt copper is in the oxidation state +1 However, the Cu (+1) present in this catalyst needs to be stabilized against moisture and to be efficiently solubilized in the reaction media, requiring in addition to avoid the disproportionation towards Cu (0) and Cu (+2). For this reason, the reaction was carried out under inert conditions and in the presence of an amine-based ligand such as PMDTA, whose main function is to stabilize the copper complex and increase the reaction rate. CuBr in combination with PMDTA ligand has been commonly used in applications of CuAAC in polymer chemistry [44].

Trace copper was removed with heterogeneous adsorbent (silica gel), reaching a final Cu concentration of 2 ppm (detected by AA), which is well below the concentration allowed by the European Medicines Agency (EMEA) pharmaceutical industry (15 ppm) [45]".

Cu Wire overcomes some of the limitations of CuBr because it provides a simple way of removing copper from the final product and can be used in subsequent reactions, which has a great importance for biological systems where high levels of copper are not allowed. In addition, the yield results obtained using Cu Wire as catalyst in our experiments, as reported in Table 1, were more promising than the ones obtained for CuBr in toluene, reaching a yield of 91.92 % at 48 h. Diaz et al. [46] reported that the terminal alkynes and internal triazoles could bind to the copper wire surface through σ or π bonding and thereby enhance the CuAAC yield values.

However, as was the case with CuBr, PMDTA was necessary in order to lead the regioselective formation of 1,4-triazol. A possible explanation for the necessity of PMDTA when using the Cu wire catalyst could be that this compound promotes the comproportionation of Cu(+2) and Cu (0) towards the active Cu (I) specie in toluene [46].The residual concentration of copper in the final click product is very low, since the solid catalyst can be removed with simple work-up techniques.

Traditional organic solvents, as toluene [27,47], could potentially cause various health and environmental problems due to their volatility and toxicity. Significant efforts have been devoted toward the development of environmentally benign process using green solvents. PEGs with MW>2000 are hard crystalline solids with melting points around 63 °C at atmospheric pressure. Sorption of scCO$_2$ into a polymer can reduce its melting temperature (Tm) significantly below the one observed at atmospheric pressure. The Tm of the mPEG-alkyne in scCO$_2$ was between 37-43 °C, implying that at 35 °C the CO2 is starting to act as a lubricant facilitating friction between the polymer chains and softening the polymer, allowing the mPEG-alkyne to start turning into a viscous liquid without the need for organic solvents or elevated temperatures [48]. In this sense, mPEG-alkyne could as main reagent and co-solvent when using scCO$_2$ as reaction media.

Considering the good physical and toxicological properties of scCO$_2$, we studied the CuAAC reaction between PEG and coumarin using different catalysts at different times and in absence of ligand or base using scCO$_2$ as reaction media, as shown Table 2.

Table 2. Yield of CuAAC reaction with different catalysts in supercritical media.

Entry	Copper Source	C/A Molar Ratio[a]	Catalyst Loading (mg)	Time (h)	Yield (%)
1	CuBr	1	7.17	24	0
2	CuBr	1	7.17	48	0
3	$Cu(CH_3COO)_2 \cdot H_2O$	0.5	5	6	11.74
4	$Cu(CH_3COO)_2 \cdot H_2O$	0.5	5	12	14.20
5	$Cu(CH_3COO)_2 \cdot H_2O$	0.5	5	24	82.32
6	$Cu(CH_3COO)_2 \cdot H_2O$	0.5	5	48	90.12
7	Cu Wire	1	3.177	24	11.60
8	Cu Wire	10	31.77	24	84.54
9	Cu Wire	100	317.73	6	18.26
10	Cu Wire	100	317.73	12	56.78
11	Cu Wire	100	317.73	24	95.96
12	Cu Wire	100	317.73	48	97.80
13	Cu Plate	10	31.77	24	15.70
14	Cu Plate	100	317.73	6	0
15	Cu Plate	100	317.73	12	13.20
16	Cu Plate	100	317.73	24	23.07
17	Cu Plate	100	317.73	48	32.66
18	Cu/β-SiC	0.1	0.32	24	16.15
19	Cu/β-SiC	0.5	1.59	6	35.20
20	Cu/β-SiC	0.5	1.59	12	82.30
21	Cu/β-SiC	0.5	1.59	24	82.59
22	Cu/β-SiC	0.5	1.59	48	90.90
23	Cu/β-SiC	1	3.2	24	91.94
24	Pre-treated Cu Wire	100	317.73	24	97.14
25	Pre-treated Cu Plate	100	317.73	24	89.70

Coumarin Azide (0.05 mmol), mPEG alkyne (0.05 mmol) at 13 MPa, 35 °C. [a]Catalyst/Alkyne molar ratio.

The entries 1-6 correspond to the powder catalysts used in $scCO_2$, CuBr and $Cu(CH_3COO)_2 \cdot H_2O$. CuBr did not show activity in the conditions studied, probably due to the mild reaction conditions and the absence of ligand. However, $Cu(CH_3COO)_2 \cdot H_2O$ exhibited an efficient behavior in the same operative reactions conditions and with half the amount of catalyst. The C/A molar ratio of $Cu(CH_3COO)_2 \cdot H_2O$ was optimized in a previous work [35] and was therefore set at a ratio of 0.5. The molar ratio for CuBr was 1. As the reaction was not carried out within 48 hours, the amount of catalyst was not further increased due to the difficulty in purification. This fact indicates that $scCO_2$ at 35 °C and 13 MPa lead to the decomposition of $Cu(CH3COO)_2 \cdot H_2O$ to different copper species with different oxidation state, such as Cu, Cu_2O and CuO, including the catalytically active specie Cu(I) in CuAAC that arises from Cu_2O.

Subsequently, three heterogeneous catalysts were employed in the CuAAC reaction in $scCO_2$, copper wire, copper plate and copper impregnated in silicon carbide pellets. The proposed mechanism for CuAAC with $scCO_2$ catalyzed by metallic copper was from Cu(I)

as could be seen in section 2. 2 and the formation of Cu(I) from metal copper is also due to the unfilled valences of the surface atom.

Both heterogeneous catalysts used in the CuAAC reaction, in $scCO_2$ and in absence of ligand showed good catalytic behavior. The entries (7-8-11, 13-16, 18-21-22) were previous experiments used to determine the optimal amount of heterogenous catalyst based on the yield obtained after 24 h. As it could be noticed in Table 2, when the amount of Cu Wire, Cu Plate and Cu/β was increased the reaction yield valued increased too. For Cu Wire and Cu Plate, the C/A molar ratio to get the maximum yield value was 100. However, for Cu/β-SiC pellets, the reaction could be optimized for a catalyst load of 0.5 C/A molar ratio, as the yield was higher than 90 %. As expected, an increase in catalyst loading is translated into an increase in the yield.

The results in Table 2 reveal that Cu Wire, Cu Plate and Cu/β-SiC were more active than $Cu(CH_3COO)_2 \cdot H_2O$ and CuBr. The yield obtained in the presence of Cu Wire was higher than those obtained with Cu Plate and Cu/β-SiC pellets. However, the amount of copper required to achieve approximately 90 % of yield was much less in Cu/β-SiC pellets than in Cu Wire. The method of purification of the residual copper in the final click product, using the heterogeneous catalyst, was a simple work-up technique (laboratory tweezers) and the residual copper in the sample did not exceed 1 ppm.

Cu Plate was even less active than $Cu(CH_3COO)_2 \cdot H_2O$, this may be due to the fact that the operating conditions using $scCO_2$ as solvent were not selective to oxidize the copper plate and therefore did not generate the Cu (+1) ions, as could be verified by the XRD in Figure 2 (b). Nevertheless, the use of the pre-treated Cu Plate improved the reaction yield. The pre-treatment for Cu Wire did not have such a significant effect on the yield of reaction. Therefore, it is concluded that the three heterogeneous catalysts considered and $scCO_2$ as reaction media offer a very promising result in the CuAAC model reaction.

2.4. Reusability of heterogeneous copper structures in $scCO_2$.

The recyclability of the heterogeneous catalyst was examined in the CuAAC model reaction as shown in Table 3. In addition, the copper leaching calculated from the weight difference was also studied. All the reactions were carried out at 35 °C and 13 MPa for 24 h in order to achieve the highest possible conversion. After each cycle the surface of the catalysts was cleaned by rinsing with Milli-Q water. The study of the lifetime and level of reusability was considered for the copper plate without pre-treatment due to the low yields obtained in the previous section.

According to Table 3, copper leaching was observed each cycle, however the leaching did not affect substantially to the CuAAC reaction yield. With respect to the Cu/β-SiC, it was only possible to reuse this catalyst up to a second cycle because the product remained attached to the pellets, blocking the access of fresh reactants to the active centres. In order to wash the catalytic surface, organic solvents (ethyl acetate) and water had to be used under an ultrasonic bath at room temperature for 30 minutes. However, from the third cycle onwards, the catalytic activity was negligible.

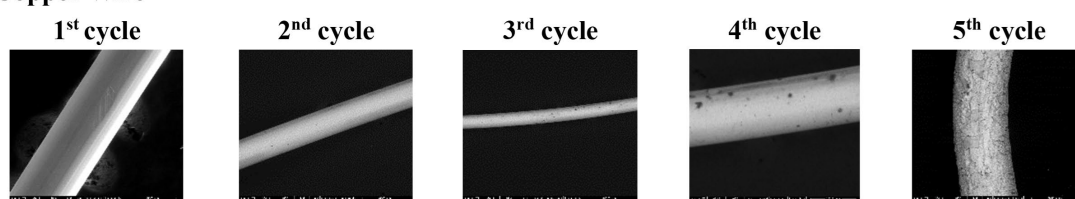**Table 2.** Reusability of heterogenous catalyst in $scCO_2$.

Cycle		1	2	3	4	5
Copper Wire	**Yield (%)**	95.9	94.7	95.1	95.4	94.2
	Copper Leaching (%)	-	1.2	6	5	3.4
Cu/β-SiC	**Yield (%)**	82.9	79.6			
	Copper Leaching (%)	-	2	-	-	-
Pre-treated CW	**Yield (%)**	97.1	86.6	85.2	25.1	-
	Copper Leaching (%)	-	2.4	5.8	7	
Pre-treated CP	**Yield (%)**	89.7	90.1	73.3	13.4	-

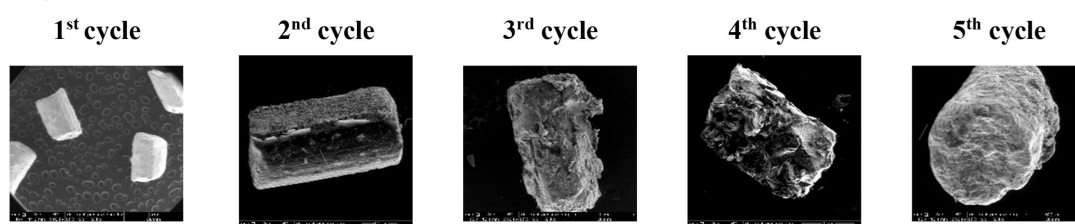|				
Copper Leaching (%)	-	7.9	12.1	5.6

The cleaning of the pre-treated catalysts was done with considerable caution because the oxide layer formed in the pre-treatment disappeared after washing, although they showed a high catalytic efficiency up to the third cycle. From this cycle onwards, the structural stability of both pre-treated catalysts was affected. In the third cycle, based on the AA analysis the amount of copper in the clicked product was 16.7 ppm, so the sample was purified using a chromatographic column of silica gel in order to remove residual copper.

To identify the stability of heterogeneous catalyst, SEM images were also obtained, as shown in Figure 7. Photographs suggest a slight but visible morphological change after five cycles, but despite these changes the overall activity of the Cu Wire still remains relatively high, not showing visible changes in catalyst structure.
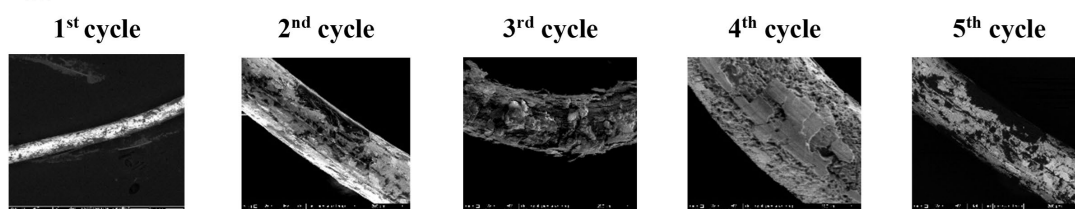
Copper Wire

1st cycle	2nd cycle	3rd cycle	4th cycle	5th cycle

Cu/ β-SiC

1st cycle	2nd cycle	3rd cycle	4th cycle	5th cycle

Copper Wire Pre-treated

1st cycle	2nd cycle	3rd cycle	4th cycle	5th cycle

Copper Plate Pre-treated

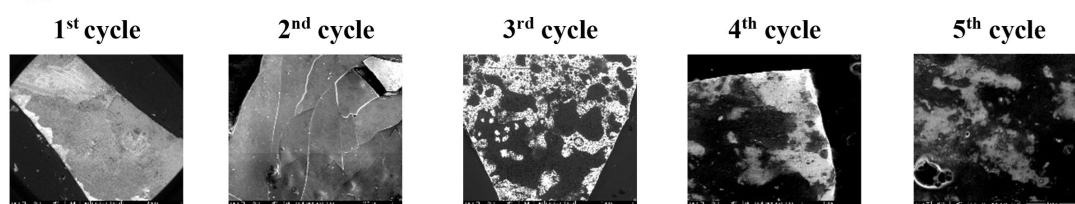| 1st cycle	2nd cycle	3rd cycle	4th cycle	5th cycle

Figure 5. SEM Images of heterogeneous catalyst in scCO$_2$ as solvent after five cycles.

The images of Cu/β-SiC pellets shown how the product adheres to the pellet making it hard to clean the catalyst for another cycle. The pre-treated catalysts exhibited severe weathering and considerable changes in their structures. In fact, the SEM images showed the weathering and fracture of copper plate from the second cycle onwards and from the third cycle for copper wire.

3. Materials and Methods

3.1. Materials.

The following materials were used to carry out the different synthesis: AMMC (synthesis was published in literature [49-52]) and methoxy mPEG-alkyne 2000 g/mol (Specific Polymers, France) were used without further purification. Copper wire with a diameter 0.25 mm, plate of copper with a thickness of 2 mm, copper (II) acetate monohydrate and copper (I) bromide were obtained from Sigma Aldrich. Silicon carbide pellets were purchased of SICAT (France). The solvents used were THF, toluene, and PMDTA which were obtained from Sigma Aldrich. Carbon dioxide was provided by Air Liquide, Spain, with a purity of 99.8 %.

3.2. Synthesis of click product in scCO$_2$.

0.05 mmol of mPEG-alkyne and 0.05 mmol of AMMC were introduced together with the corresponding amount of catalyst in a high-pressure reactor, in absence of ligand. Once the reactor was hermetically sealed, scCO$_2$ was pumped out until reaching a pressure of 13 MPa and the reactor was heated until 35 °C. Once the reaction was complete, the heating was switched off and the reactor depressurized with a flow rate of 3 L/min.

3.3. Synthesis of click product at atmospheric pressure.

The procedure for synthesizing the click product at atmospheric pressure starts with the introduction of the reagents into a 250 mL flask and then the mixture was stirred at 80 °C. The reagents added were coumarin azide (0.05 mmol), mPEGalkyne (0.05 mmol) and PMDTA (0.05 mmol), using 20 mL of anhydrous Toluene as solvent under nitrogen inert atmosphere. Catalyst/alkyne molar ratio was fixed at 1 for the CuBr catalyst and at 100 for the Cu Wire catalyst. Once the reaction is finished, a purification of the final product was carried out.

3.4. Click product characterization.

Gel permeation chromatography (GPC) analyses were performed with a Viscotek chromatograph with two columns (Styragel HR2 and Styragel HR0.5) at 35 °C with a flow of 1 mL/min and THF as eluent. The calibration curves for GPC analysis were obtained with poly (ethylene glycol) standards (from Waters). All reactions were monitored by GPC, from which the rate of loss of starting reagents was determined and yield of reaction for each particular CuAAC reaction were calculated based on the normalized weight distribution form GPC traces (GPCs are included in Supplementary Material, Figure S4-S7). In addition, to characterise the final product, nuclear magnetic resonance (NMR), matrix-assisted laser desorption/ionization time-of-flight mass spectrometry (MALDI TOF) and Fourier-transform infrared spectroscopy (FTIR) were carried out and the spectra were included in the Supplementary Material (Figure S1-S3) [33]. The amount of copper in the product after reaction and after purification was determined by atomic absorption spectrophotometry (AA), with an error of ±1 %.

3.5. Synthesis Cu/β-SiC.

Cu/β-SiC was prepare by the traditional impregnation method. Firstly, the support was placed in a glass vessel and kept under vacuum at room temperature (~25 °C) for 2 h to remove water and other impurities adsorbed on the structure. Secondly, an aqueous solution of Cu(CH$_3$COO)$_2$·H$_2$O was poured drop by drop over the support, with the appropriate amount of metal precursor in order to obtain catalysts with Cu loadings of 6, 3 and 0.6 wt. %. Thirdly, the solvent was removed under vacuum at 90 °C for 2 h and the pellets were dried at 120 °C overnight. After drying, the samples were calcined under N2 (10 °C/min) at 600 °C for 4 h.

3.6. Pre-treatment of Cu Wire and Cu Plate.

Previously to the pre-treatment, the sample reducibility was studied by H_2-TPR. Analyses were conducted in a commercial Micromeritics AutoChem 2950 HP analyser unit with a thermal conductivity detector (TCD). After loading 0.13 g, the sample was reduced by a 5 v/v. % H_2 (10 mL/min) at a heating rate of 5 °C/min up to 900 °C. Then, the sample was cooled down and an oxidation step started, using synthetic air (10 mL/min) and a heating rate of 5 °C/min up to 900 °C. After oxidation, the reduction step was repeated to check the formation of the different copper oxides.

Pre-treatment of copper wire and copper plate was carried out with the main objective to increase the reaction rate by generation of Cu (I) species on the surface of the wire and plate. Samples were pre-treated in a tubular quartz reactor (75 cm length divided at the middle into two parts with two different diameters, 1.5 and 0.7 cm, respectively). The feed systems consist in three lines, for the feeding of O_2/N_2 (synthetic air, 99.99 % purity) used for oxidizing the sample, H_2 (99.99 % purity) used to reduce the sample and N_2 (99.99 % purity) used to keep inert the sample. After loading the sample, the sample is heated from room temperature to 400 °C at 6.67 °C/min in a continuous flow of synthetic air stream. After reaching 400 °C, the sample was kept at these conditions for 120 minutes with a synthetic air stream (10 mL/min). In the third stage the temperature is decreased to 200 °C while a stream of nitrogen (50 mL/min) is passed through the reactor with a rate of 10 °C/min. Finally, a hydrogen stream (10 mL/min) is passed through for 30 min.

3.7. Catalyst characterization.

The amount of copper in the catalyst was determined by AA, with an error of ±1 %, using a SPECTRAA 220FS. All catalysts were also characterized before and after reactions by X-ray diffraction (XRD), with a Philips PW-1710 instrument, using Ni-filtered Cu Kα radiation ($\lambda = 1.54056$ Å). The samples were scanned at a rate of 0.02°·step^{-1} over the range $20° \leq 2\theta \leq 100°$ (scan time 4 s·per step) and the diffractograms were compared with the JCPDS-ICDD references. In addition, the Cu Wires, the Cu plates and the synthesized catalyst were depicted by means of scanning electron microscopy (SEM) by using a FEI QUANTA 250 with a wolfram filament operating at a working potential of 10 kV (FEI Company).

3.8. Purification steps.

The purification process of the final product depended on the solvent (Toluene or scCO$_2$) and catalyst (Cu Wire, Cu Plate, CuBr, Cu(CH$_3$COO)$_2$·H$_2$O and Cu/β-SiC). The purification of the product obtained using Toluene as reaction media started with the solvent removal using a rotary evaporator. Once click product has been removed from the solvent traces, the next steps focused on the elimination of the catalyst. CuBr and Cu(CH$_3$COO)$_2$·H$_2$O were removed through a chromatographic column whereas copper wire, copper plate and Cu/β-SiC were removed from the final product using laboratory tweezers. When scCO$_2$ was used as solvent only the catalyst elimination step was needed in the purification process.

4. Conclusions

The CuAAC reaction has been widely used in the synthesis of polymers. In this work, it has been demonstrated that the ligand, solvent, copper catalyst and the interaction between catalyst and solvent had a significant effect on the CuAAC reaction. XRD showed the modification of the oxidation state of Cu(CH$_3$COO)$_2$·H$_2$O and Cu Wire in scCO$_2$, however CuBr, Cu Plate and Cu/β-SiC suffer no change. In addition, a pre-treatment procedure for Cu Wire and Cu Plate was developed based on TPR results, what increase the amount of Cu (+1) species on the surface of both catalysts, whats were confirmed byXRD spectra and SEM images.

Activity in the CuAAC reaction has been compared using toluene and scCO$_2$ as reaction media and different types of catalysts. From the study of this comparison, it can be

concluded that when toluene is used as solvent the yield values exhibited significant increase using Cu Wire instead of CuBr. In addition, PMDTA was necessary in order to carried out the reaction. In the case of using $scCO_2$ as reaction media, CuAAC was carried out properly with $Cu(CH_3COO)_2 \cdot H_2O$, Cu Wire, Pre-treated Cu Wire, Pre-treated Cu Plate and Cu/β-SiC as catalysts. However, with Cu Plate the yield value was low and with CuBr there was not conversion at all.

The recovery of the catalysts was studied, and it was found that Cu Wire could be used up to 5 cycles, Pre-treated Cu Wire up to 3 and Pre-treated Cu Plate and Cu/β-SiC up to the second cycle without important decrease of the activity. The relationships of various aspects such as solvents and catalyst proposed here suggest further modifications that can be made to improve the performance of the CuAAC reaction, confirming that the use of eco-friendly $scCO_2$ as reaction media the most interesting alternative to organic solvents.

Supplementary Material: The following supporting information can be downloaded at: www.mdpi.com/xxx/s1. Figure S 1. (up) FTIR: (a) BMMC, (b) AMMC (down) ^{1}H-NMR Spectrum of AMMC. Figure S 2: FTIR comparative between starting reagents mPEG-alkyne and AMMC (azido-coumarin) and click product, coumarin-PEG (CouPEG). Figure S 3: ^{1}H NMR of coumarin azide and click product. Figure S 4: MALDI TOFF MS of a) starting mPEG-alkyne and b) click product CouPEG. Figure S 5: GPC of CuAAC reaction at 80 °C, inert atmosphere and Toluene with Cu Wire. Figure S 6: GPC of CuAAC reaction at 80 °C, inert atmosphere and toluene with CuBr. Figure S 7: GPC of CuAAC reaction corresponding to the preliminary study in $scCO_2$ at 13 MPa and 35 °C. a) Cu Wire at C/A=1, 10 and 100, b) Cu Plate C/A=10, 100, Cu/β-SiC, C/A=0.1, 0.5 and 1. Figure S 7: GPC of CuAAC reaction corresponding to the assess of different catalysts in $scCO_2$ at 35 °C and 13 MPa. a) Cu Wire (6, 12, 24, 48 h), b) Cu Plate (12, 24, 48 h), c) Cu/β-SiC (6, 12, 24, 48 h), d) Pre-treated Cu Wire (24 h), e) Pre-treated Cu Plate (24 h) and f) $Cu(OAc)_2 \cdot H_2O$ (6, 12, 24 and 48 h).

Author Contributions: Conceptualization, visualization, formal analysis, writing—original draft preparation, writing—review and editing, S.L., J.M.G.-V., M.J.R., J.F.R., I.G. and M.T.G.; methodology, software, validation, investigation, data curation, S.L. resources, supervision, project administration, J.M.G.-V., M.J.R., J.F.R., I.G. and M.T.G. All authors have read and agreed to the published version of the manuscript.

Conflicts of Interest: The authors declare no conflict of interest.

References

1. R. Huisgen, G. Mloston, E. Langhals, The first two-step 1,3-dipolar cycloadditions: non-stereospecificity, *J. Am. Chem. Soc.* **1986** *108* pp.6401–6402. https://doi.org/10.1021/ja00280a053.

2. V. V. Rostovtsev, L.G. Green, V. V. Fokin, K.B. Sharpless, A stepwise huisgen cycloaddition process: Copper(I)-catalyzed regioselective "ligation" of azides and terminal alkynes, *Angew. Chemie - Int. Ed.* **2002** *41* pp.2596–2599. https://doi.org/10.1002/1521-3773(20020715)41:14<2596::AID-ANIE2596>3.0.CO;2-4.

3. H.C. Kolb, M.G. Finn, K.B. Sharpless, Click Chemistry: Diverse Chemical Function from a Few Good Reactions, *Angew. Chemie Int. Ed.* **2001** *40* pp.2004–2021. https://doi.org/10.1002/1521-3773(20010601)40:11<2004::AID-ANIE2004>3.0.CO;2-5.

4. V. V Rostovtsev, L.G. Green, V. V Fokin, K.B. Sharpless, A Stepwise Huisgen Cycloaddition Process: Copper(I)-Catalyzed Regioselective "Ligation" of Azides and Terminal Alkynes, *Angew. Chemie Int. Ed.* **2002** *41* pp.2596–2599. https://doi.org/10.1002/1521-3773(20020715)41:14<2596::AID-ANIE2596>3.0.CO;2-4.

5.   H.C. Kolb, K.B. Sharpless, The growing impact of click chemistry on drug discovery, *Drug Discov. Today*. **2003** *8* pp.1128–1137. https://doi.org/10.1016/S1359-6446(03)02933-7.

6.   M. van Dijk, D.T.S. Rijkers, R.M.J. Liskamp, C.F. van Nostrum, W.E. Hennink, Synthesis and Applications of Biomedical and Pharmaceutical Polymers via Click Chemistry Methodologies, *Bioconjug. Chem.* **2009** *20* pp.2001–2016. https://doi.org/10.1021/bc900087a.

7.   V. Crescenzi, L. Cornelio, C. Di Meo, S. Nardecchia, R. Lamanna, Novel Hydrogels via Click Chemistry: Synthesis and Potential Biomedical Applications, *Biomacromolecules*. **2007** *8* pp.1844–1850. https://doi.org/10.1021/bm0700800.

8.   K. Nwe, M. Brechbiel, Growing Applications of "Click Chemistry" for Bioconjugation in Contemporary Biomedical Research, *Cancer Biother. Radiopharm.* **2009** *24* pp.289–302. https://doi.org/10.1089/cbr.2008.0626.

9.   Rostovtsev, V.V., Green, L.G., Fokin, V.V. and Sharpless, K.B.. A Stepwise Huisgen Cycloaddition Process: Copper(I)-Catalyzed Regioselective "Ligation" of Azides and Terminal Alkynes. *Angewandte Chemie International Edition*. **2002**, 41: 2596-2599. https://doi.org/10.1002/1521-3773(20020715)41:14<2596::AID-ANIE2596>3.0.CO;2-4

10.   Binder, W.H. and Sachsenhofer, R. 'Click' Chemistry in Polymer and Material Science: An Update. *Macromol. Rapid Commun.*, **2008**, 29: 952-981. https://doi.org/10.1002/marc.200800089.

11.   A.R. Ellanki, A. Islam, V.S. Rama, R.P. Pulipati, D. Rambabu, G. Rama Krishna, C. Malla Reddy, K. Mukkanti, G.R. Vanaja, A.M. Kalle, K. Shiva Kumar, M. Pal, Solvent effect on copper-catalyzed azide–alkyne cycloaddition (CuAAC): Synthesis of novel triazolyl substituted quinolines as potential anticancer agents, *Bioorg. Med. Chem. Lett.* **2012** *22* pp.3455–3459. https://doi.org/10.1016/j.bmcl.2012.03.091.

12.   S. Kazarian, Polymer Processing with Supercritical Fluids, *Polym. Sci.* **2000** *42* pp.78-101. https://doi.org/10.1002/3527606726.CH10

13.   Y.-T. Shieh, J.-H. Su, G. Manivannan, P. Lee, S. Sawan, W. Spall, Interaction of supercritical carbon dioxide with polymers. I. Crystalline polymers, *J. Appl. Polym. Sci.* **1996** *59* pp.695–705. https://doi.org/10.1002/(SICI)1097-4628(19960124)59:4<695::AID-APP15>3.0.CO;2-P.

14.   D. Prajapati, M. Gohain, Recent Advances in the Application of Supercritical Fluids for Carbon—Carbon Bond Formation in Organic Synthesis, *Tetrahedron*. **2004** *60* pp.815–833. https://doi.org/10.1016/j.tet.2003.10.075.

15.   R.S. Oakes, A.A. Clifford, C.M. Rayner, The use of supercritical fluids in synthetic organic chemistry, *J. Chem. Soc., Perkin Trans. 1*. **2001** pp.917–941. https://doi.org/10.1039/B101219N.

16.   B. Grignard, S. Schmeits, R. Riva, C. Detrembleur, P. Lecomte, C. Jérôme, First example of "click" copper(I) catalyzed azide-alkyne cycloaddition in supercritical carbon dioxide: application to the functionalization of aliphatic polyesters, *Green Chem. - GREEN CHEM.* **2009** *11*. https://doi.org/10.1039/b822924d.

17.   B. Grignard, C. Calberg, C. Jerome, C. Detrembleur, "One-pot" dispersion ATRP and alkyne-azide Huisgen's 1,3-dipolar cycloaddition in supercritical carbon dioxide: Towards the formation of functional microspheres, *J. Supercrit. Fluids*. **2010** *53* pp.151–155. https://doi.org/10.1016/j.supflu.2009.12.014.

18.   W. Zhang, X. He, B. Ren, Y. Jiang, Z. Hu, Cu(OAc)$_2$·H$_2$O—an efficient catalyst for Huisgen-click reaction in supercritical carbon dioxide, *Tetrahedron Lett.* **2015** *56* pp.2472–2475. https://doi.org/https://doi.org/10.1016/j.tetlet.2015.03.102.

19.   E. Gracia, M.T. García, A.M. Borreguero, A. De Lucas, I. Gracia, J.F. Rodríguez, Functionalization and optimization of PLA with coumarin via click chemistry in supercritical CO$_2$, *J. CO$_2$ Util.* **2017** *20* pp.20–26. https://doi.org/10.1016/j.jcou.2017.04.008.

20.   E. Haldón, M.C. Nicasio, P.J. Pérez, Copper-catalysed azide–alkyne cycloadditions (CuAAC): an update, *Org. Biomol. Chem.* **2015** *13* pp.9528–9550. https://doi.org/10.1039/C5OB01457C.

21.   S. Chassaing, V. Bénéteau, P. Pale, When CuAAC 'Click Chemistry' goes heterogeneous, *Catal. Sci. Technol.* **2016** *6* pp.923–957. https://doi.org/10.1039/C5CY01847A.

22.   S. Neumann, M. Biewend, S. Rana, W.H. Binder, The CuAAC: Principles, Homogeneous and Heterogeneous Catalysts, and

Novel Developments and Applications, *Macromol. Rapid Commun.* **2020** *41* pp.190-359. https://doi.org/10.1002/marc.201900359.

23.   G. Hu, J. Chen, Y. Fan, H. Zhou, K. Guo, Z. Fang, L. Xie, L. Wang, Y. Wang, A promoted copper-catalysed Azide-alkyne cycloaddition (CuAAC) for broad spectrum peptide-engineered implants, *Chem. Eng. J.* **2022** *427* pp.130918. https://doi.org/https://doi.org/10.1016/j.cej.2021.130918.

24.   M. Meldal, F. Diness, Recent Fascinating Aspects of the CuAAC Click Reaction, *Trends Chem.* **2020** *2* pp.569–584. https://doi.org/10.1016/j.trechm.2020.03.007.

25.   Q. Wang, T.R. Chan, R. Hilgraf, V. V Fokin, K.B. Sharpless, M.G. Finn, Bioconjugation by Copper(I)-Catalyzed Azide-Alkyne [3 + 2] Cycloaddition, *J. Am. Chem. Soc.* **2003** *125* pp.3192–3193. https://doi.org/10.1021/ja021381e.

26.   T.R. Chan, R. Hilgraf, K.B. Sharpless, V. V Fokin, Polytriazoles as Copper(I)-Stabilizing Ligands in Catalysis, *Org. Lett.* **2004** *6* pp.2853–2855. https://doi.org/10.1021/ol0493094.

27.   P.L. Golas, N. V Tsarevsky, B.S. Sumerlin, K. Matyjaszewski, Catalyst Performance in "Click" Coupling Reactions of Polymers Prepared by ATRP: Ligand and Metal Effects, *Macromolecules*. **2006** *39* pp.6451–6457. https://doi.org/10.1021/ma061592u.

28.   K. Fauché, F. Cisnetti, Magnetic Fe_3O_4 nanoparticles bearing CuI-NHC complexes by an "auto-click" strategy, *Inorganica Chim. Acta*. **2021** *520* pp.120312. https://doi.org/10.1016/j.ica.2021.120312.

29.   S. Chassaing, M. Kumarraja, A. Sani Souna Sido, P. Pale, J. Sommer, Click Chemistry in CuI-zeolites: The Huisgen [3 + 2]-Cycloaddition, *Org. Lett.* **2007** *9* pp.883–886. https://doi.org/10.1021/ol0631152.

30.   S. Parveen, G.K Gurjaspreet, S. Jandeep, S. Harminder, Robust and Versatile Cu(I) metal frameworks as potential catalysts for azide-alkyne cycloaddition reactions: *Review, Mol. Cat.*, **2021** *504* pp.111432. https://doi.org/10.1016/j.mcat.2021.111432.

31.   S. Gurjaspreet, S. Jasbhinder, S. Akshpreet, S. Jandeep, K. Manoj, G. Kshitiz, C. Sanjay. Synthesis, characterization and antibacterial studies of schiff based 1,2,3-triazole bridged silatranes, *Journal of Organometallic Chemistry*, **2018**, *871*, pp. 21-27. https://doi.org/10.1016/j.jorganchem.2018.06.024.

32.   Y. Jiang, X. He, W. Zhang, X. Li, N. Guo, Y. Zhao, G. Xu, W. Li, Metallic copper wire: a simple, clear and reusable catalyst for the CuAAC reaction in supercritical carbon dioxide, *RSC Adv.* **2015** *5* pp.73340–73345. https://doi.org/10.1039/C5RA11797F.

33.   E. Gracia, M.T. García, A. [De Lucas], J.F. Rodríguez, I. Gracia, Copper wire as a clean and efficient catalyst for click chemistry in supercritical CO_2, *Catal. Today*. **2018**. https://doi.org/10.1016/j.cattod.2018.12.021.

34.   G. Behl, M. Sikka, A. Chhikara, M. Chopra, PEG-coumarin based biocompatible self-assembled fluorescent nanoaggregates synthesized via click reactions and studies of aggregation behavior, *J. Colloid Interface Sci.* **2014** *416* pp.151–160. https://doi.org/10.1016/j.jcis.2013.10.057.

35.   S. López, I. Gracia, M.T. García, J.F. Rodríguez, M.J. Ramos, Synthesis and Operating Optimization of the PEG Conjugate via CuAAC in scCO$_2$, *ACS Omega*. **2021**. https://doi.org/10.1021/acsomega.0c05466.

36.   S.A. Alterovitz, J.A. Woollam, - Cubic Silicon Carbide (β-SiC), in: E.D. Palik (Ed.), Handb. Opt. Constants Solids, Academic Press, Burlington, **1997**: pp. 705–707. https://doi.org/10.1016/B978-012544415-6.50074-1.

37.   J.M. García-Vargas, J.L. Valverde, J. Díez, P. Sánchez, F. Dorado, Preparation of Ni–Mg/β-SiC catalysts for the methane tri-reforming: Effect of the order of metal impregnation, *Appl. Catal. B Environ.* **2015** *164* pp.316–323. https://doi.org/10.1016/j.apcatb.2014.09.044.

38.   D.L. Nguyen, P. Leroi, M.J. Ledoux, C. Pham-Huu, Influence of the oxygen pretreatment on the CO2 reforming of methane on Ni/β-SiC catalyst, *Catal. Today*. **2009** *141* pp.393–396. https://doi.org/10.1016/j.cattod.2008.10.019.

39.   P. de Meester, S.R. Fletcher, A.C. Skapski, Refined crystal structure of tetra-mu-acetato-bisaquodicopper(II), *J. Chem. Soc. Dalt. Trans. Inorg. Chem.* **1973** *1973* pp.2575–2578. https://doi.org/10.1039/DT9730002575

40.   M. Herbert, F. Montilla, A. Galindo, Supercritical carbon dioxide, a new medium for aerobic alcohol oxidations catalysed by

copper-TEMPO, *Dalt. Trans.* **2010** *39* pp.900–907. https://doi.org/10.1039/B914788H.

41. K. Mathew, C. Zheng, D. Winston, C. Chen, A. Dozier, J.J. Rehr, S.P. Ong, K.A. Persson, High-throughput computational X-ray absorption spectroscopy, *Sci. Data*. **2018** *5* pp.180151. https://doi.org/10.1038/sdata.2018.151.

42. M. Yang, J.J. Zhu, J.J. Li, Cubic assembly composed of CuBr nanoparticles, *J. Cryst. Growth*. **2004** *267* pp.283–287. https://doi.org/10.1016/j.jcrysgro.2004.03.042.

43. E. Sahle-Demessie, M.A. Gonzalez, J. Enriquez, Q. Zhao, Selective Oxidation in Supercritical Carbon Dioxide Using Clean Oxidants, *Ind. Eng. Chem. Res.* **2000** *39* pp.4858–4864. https://doi.org/10.1021/ie000175h.

44. M. Meldal, Polymer "Clicking" by CuAAC Reactions, *Macromol. Rapid Commun.* **2008** *29* pp.1016–1051. https://doi.org/10.1002/marc.200800159.

45. ICH Q3D Elemental impurities | European Medicines Agency, n.d. https://www.ema.europa.eu/en/ich-q3d-elemental-impurities (accessed November 18, 2021).

46. D. Díaz, S. Punna, P. Holzer, A.K. McPherson, K.B. Sharpless, V. V Fokin, M.G. Finn, Click chemistry in materials synthesis. 1. Adhesive polymers from copper-catalyzed azide-alkyne cycloaddition, *J. Polym. Sci. Part A Polym. Chem.* **2004** *42* pp.4392–4403. https://doi.org/10.1002/pola.20330.

47. C.A. Bell, Z. Jia, S. Perrier, M.J. Monteiro, Modulating catalytic activity of polymer-based cuAAC "click" reactions, *J. Polym. Sci. Part A Polym. Chem.* **2011** *49* pp.4539–4548. https://doi.org/10.1002/pola.24896.

48. S. López, M.J. Ramos, J.M. García-Vargas, M.T. García, J.F. Rodríguez, I. Gracia, Carbon dioxide sorption and melting behaviour of mPEG-alkyne, *J. Supercrit. Fluids*. **2021** *171* pp.105182. https://doi.org/10.1016/j.supflu.2021.105182.

49. C. Oh, I. Yi, K.P. Park, Nucleophilic vinylic substitution of halocoumarins and halo-l,4-naphthoquinones with morpholine, *J. Heterocycl. Chem.* **1994** *31* pp.841–844. https://doi.org/10.1002/jhet.5570310426.

50. K. Sivakumar, F. Xie, B.M. Cash, S. Long, H.N. Barnhill, Q. Wang, A Fluorogenic 1,3-Dipolar Cycloaddition Reaction of 3-Azidocoumarins and Acetylenes, *Org. Lett.* **2004** *6* pp.4603–4606. https://doi.org/10.1021/ol047955x.

51. R.A. Kusanur, M. V Kulkarni, G.M. Kulkarni, S.K. Nayak, T.N. Guru Row, K. Ganesan, C.-M. Sun, Unusual anisotropic effects from 1,3-dipolar cycloadducts of 4-azidomethyl coumarins, *J. Heterocycl. Chem.* **2010** *47* pp.91–97. https://doi.org/10.1002/jhet.273.

52. C.S. Chaurasia, J.M. Kauffman, Synthesis and fluorescent properties of a new photostable thiol reagent "BACM," *J. Heterocycl. Chem.* **1990** *27* pp.727–733. https://doi.org/10.1002/jhet.5570270347.